MedCrave Step into the World of Research
MedCrave Online Journal of Applied Bionics and Biomechanics

Research Article

Open Access

Oscillatory flow of a bio-magnetic viscoelastic fluid in a channel with stretching walls

Abstract

To understand the role of the magnetic field on blood flow in the therapeutic heating of tumors, this study investigates the flow characteristics of a biomagnetic viscoelastic fluid within a channel bounded by stretched walls that are undergoing an oscillatory motion. Under the influence of an externally applied magnetic field generated by a magnetic dipole, blood is modeled as a non-Newtonian fluid using Walter's liquid B model, and its magnetization is assumed to vary linearly with temperature, reflecting ferrofluid behavior. The wall motion is prescribed as oscillatory with a specified velocity profile. Through appropriate similarity transformations, the governing partial differential equations are transformed into a set of coupled, nonlinear ordinary differential equations, which are solved numerically using a finite difference method in conjunction with Newton's linearization technique. The resulting simulations provide detailed insights into velocity, pressure, and temperature fields, as well as skin friction and heat transfer rates. Parametric analysis reveals the significant influence of magnetic field strength and viscoelastic properties on the flow dynamics. The findings suggest that the magnetic dipole configuration could play a crucial role in controlling blood flow in arteries, with potential applications in targeted hyperthermia-based cancer therapies.

Keywords: blood flow, viscoelasticity, flow oscillation, stretchable vessel walls

Volume 10 Issue 1 - 2026

Raju Haldar,[1] Gopal Chandra Shit,[2] JC Misra[3]
[1]Mathematics Department, Sammilani Mahavidyalaya, India
[2]Mathematics Department, Jadavpur University, India
[3]Mathematics Department, Indian Institute of Engineering Science and Technology, India

Correspondence: Gopal Chandra Shit, Mathematics Department, Jadavpur University, Kolkata, India, Tel +918335022347

Received: April 02, 2026 | **Published:** May 18, 2026

Introduction

A ferromagnetic fluid is a stable colloidal suspension composed of nanoscale magnetic particles uniformly dispersed within a liquid carrier. The behavior of ferrofluids is heavily influenced by the thermal Brownian motion of the suspended particles and the permanent magnetization of each particle.[1] One notable characteristic of ferrofluids is their temperature-dependent magnetization, which, when coupled with thermomagnetic effects, enhances their utility in a wide range of practical applications[2] in biomedical engineering, particularly in understanding and controlling blood flow under externally applied magnetic fields. The mathematical model of oscillatory biomagnetic viscoelastic blood flow in a channel with stretching walls provides useful insights into how magnetic dipole–induced fields can regulate velocity, temperature distribution, and wall shear stress in arterial flows. Such control mechanisms are especially relevant in magnetic hyperthermia-based cancer therapy, where localized heating of tissues is required without damaging surrounding healthy regions. In addition, the results can contribute to the development of targeted magnetic drug delivery systems,[3] improved regulation of microcirculatory flow, and the design of biomedical devices that involve ferrofluid-assisted transport and thermal management.

Understanding the behavior of ferrofluids in the presence of an applied magnetic field, such as that produced by a magnetic dipole, is crucial for advancing the field of biomagnetic fluid dynamics (BFD), which specifically considers blood as a biomagnetic fluid. While magnetohydrodynamics (MHD) primarily deals with electrically conductive fluids, the BFD model distinguishes itself by not accounting for induced currents from polarization and magnetization, resulting in minimal Lorentz forces. Instead, in BFD, the forces due to magnetization and polarization are the dominant ones. BFD is an emerging area within fluid mechanics that examines the behavior of biological fluids in the presence of magnetic fields. Blood, the most prominent example of a biomagnetic fluid, contains red blood cells rich in hemoglobin, an iron oxide compound abundant in mature red blood cells. Studies have shown that red blood cells tend to align with their disk planes parallel to the applied magnetic field.[4–7] Furthermore, blood displays diamagnetic properties when oxygenated and paramagnetic properties when deoxygenated.[8] Consequently, blood can be classified as a magnetic material, and depending on its oxygenation status, it can be considered either a diamagnetic or paramagnetic fluid.[9]

Mathematical modeling plays a pivotal role in understanding the complex flow behavior of biomagnetic fluids in the presence of externally applied magnetic fields. These models often extend the classical Stokes framework by incorporating magnetization effects, in addition to the fundamental thermodynamic variables.[10,11] Magnetization, defined as the magnetic moment per unit volume, represents the degree to which a magnetic material becomes magnetized. It is inherently dependent on both the applied magnetic field strength and temperature, and is quantitatively determined by the product of the number of magnetic dipoles per unit volume and the magnetic moment of each dipole. Numerous studies have examined the dynamics of biomagnetic fluid flow (BFD) under various physical influences. For instance, the effects of thermal radiation and nanoparticle dispersion on biomagnetic flows over stretching surfaces have been widely explored.[12–17] Tzirtzilakis and Kafoussias[18,19] investigated the behavior of a heated ferrofluid over a linearly stretching sheet under the action of a magnetic dipole-generated field. In a subsequent study, Tzirtzilakis et al.,[20] analyzed turbulent biomagnetic fluid flow in a rectangular channel subjected to a localized magnetic field. Their findings revealed the formation of two counter-rotating vortices near the region of magnetic influence, which significantly altered the overall flow field. Advancements in modeling have also led to the integration of ferrohydrodynamic (FHD) and magnetohydrodynamic (MHD) principles to capture the combined effects of magnetization and electrical conductivity in biological fluids, such as blood. Habibi et al.,[21] developed a model to study blood flow in a two-dimensional channel exposed to a spatially varying magnetic field, accounting for both FHD and MHD effects. Andersson and Valnes[22] studied the flow of a heated ferrofluid over a stretching sheet under the influence of a magnetic dipole, noting that the applied magnetic field generally

decelerates the fluid motion and leads to increased skin friction along the surface. Despite these contributions, most prior investigations have focused on homogeneous, Newtonian fluid models, which fail to accurately capture the non-Newtonian characteristics of biological fluids, such as blood. In reality, blood exhibits viscoelastic properties that significantly influence its flow dynamics, particularly under physiological and pathological conditions. This gap highlights the need for more comprehensive models that incorporate both magnetization effects and the viscoelastic nature of blood to better understand and predict biomagnetic fluid behavior in biomedical applications.

Thurston, Fukada and Kaibara, and Stoltz and Lucius demonstrated that blood can exhibit viscoelastic behavior under certain physiological conditions.[23–25] This behavior arises from the intrinsic viscoelasticity of individual erythrocytes and the complex internal microstructures that form through cellular interactions and aggregation. To better capture these non-Newtonian characteristics, Misra et al.,[26–28] developed mathematical models to analyze the flow of biomagnetic viscoelastic fluids over stretching surfaces and within channels bounded by stretching walls, considering the influence of magnetic fields generated by magnetic dipoles. Several studies have expanded on these ideas within the framework of magnetohydrodynamics (MHD). Researchers have extensively examined the flow of non-Newtonian viscoelastic fluids[29–31] and power-law fluids[32,33] past linearly stretching sheets in the presence of magnetic fields. These investigations offer valuable insights into the interaction of magnetic fields with complex fluids. Furthermore, Misra et al.,[34,35] investigated the steady flow of an incompressible, second-grade, electrically conducting fluid in a channel subjected to a uniform transverse magnetic field, providing foundational work with significant implications for biomedical engineering. Their later studies[36] presented both analytical and numerical analyses of blood flow through channels with stretching walls under the influence of a magnetic field, highlighting the role of fluid elasticity and magnetization in modifying flow patterns. Nadeem et al.,[37] investigated the effects of heat and mass transfer on Newtonian biomagnetic blood flow through a tapered, porous, stenosed artery, thereby contributing to a better understanding of pathological flow conditions. Ramachandra Rao et al.,[38] examined the oscillatory MHD flow of oxygenated blood in a channel exposed to magnetic fields, thereby enhancing the understanding of pulsatile blood flow and its modulation by external magnetic forces.

Hyperthermia treatment has recently emerged as an effective method in cancer therapy. The objective of this treatment is to elevate the temperature of targeted tissues to a range above the cytotoxic threshold (typically between 42°C and 45°C) while minimizing damage to surrounding healthy tissues.[39] The temperature distribution within living tissues is primarily affected by factors such as the thermal conductivity of the tissues, the sources of heat, the characteristics of power deposition patterns, and heat transfer due to blood flow.[40] Numerous studies have investigated the impact of oscillatory flow on the velocity profile, but few have explored its effects on heat transfer.[41,42] Craciunescu and Clegg[43] investigated a numerical study to analyze the influence of blood velocity pulsations on temperature distribution, providing valuable insights into the thermal dynamics of blood flow in medical applications.

This study presents an analysis of the unsteady flow of a biomagnetic viscoelastic fluid in a channel with oscillating and stretchable walls, modeling blood as a non-Newtonian fluid based on Walter's liquid B theory. The primary aim was to investigate the oscillatory behavior of blood flow under the combined influence of wall motion and an externally applied magnetic field generated by a magnetic dipole. The governing equations were first formulated analytically and then solved numerically using a finite difference method. The results highlight the critical roles played by magnetization and viscoelastic effects in shaping the velocity and temperature profiles, as well as influencing skin friction and heat transfer characteristics. Notably, the application of a magnetic field can be used to modulate blood flow behavior, with the potential to enhance therapeutic outcomes. The findings of this investigation have significant implications in biomedical engineering, particularly in the context of controlled blood flow during surgical procedures and in the advancement of hyperthermia-based cancer treatments. Furthermore, the insights gained could contribute to the development of targeted magnetic drug delivery systems, offering improved precision in the localized treatment of diseases.

Problem description and mathematical model

Consider the unsteady, two-dimensional flow of an incompressible viscoelastic biomagnetic fluid, governed by Walter's liquid B fluid model, through a channel with flexible walls located at $y = \pm h$ (as illustrated in Figure 1). The flow is described using Cartesian coordinates (x, y), where the x-axis is along the centerline of the channel, parallel to its walls, and the y-axis extends in the transverse direction. It is assumed that the flow is symmetric with respect to the x-axis.

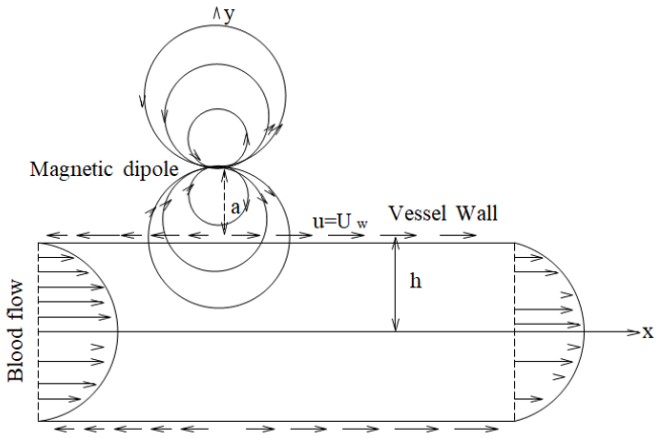

Figure 1 Graphical representation of the problem in which walls are stretchable due to the elastic response of the blood vessels.

The flow is induced by the linear stretching of an adjacent boundary, which is subjected to two equal and opposite forces along the x-axis while keeping the origin fixed. This arrangement generates a periodic velocity for each wall with a magnetic dipole placed at a distance an above the channel wall, while the wall itself is maintained at a constant temperature T_w.

We examine the time-dependent, two-dimensional motion of an incompressible, viscoelastic biomagnetic fluid within a channel bounded by flexible walls situated at $y = \pm h$, as depicted in Figure 1. The behavior of the fluid is modeled using Walter's liquid B framework. A Cartesian coordinate system (x, y), is employed, where the x-axis lies along the channel's centerline and runs parallel to the walls, while the y-axis represents the direction perpendicular to the flow. The system is considered to be symmetric about the x-axis.

The motion is initiated by the linear extension of one boundary, which is driven by a pair of equal and opposite forces acting along the x-direction, with the origin remaining stationary. This setup results in a time-periodic velocity profile at each boundary. Additionally, a magnetic dipole is positioned at a vertical distance a above the channel, and the wall surfaces are held at a uniform temperature T_w.

Citation: Haldar R, Shit GC, Misra JC. Oscillatory flow of a bio-magnetic viscoelastic fluid in a channel with stretching walls. *MOJ App Bio Biomech.* 2026;10(1):60–61. DOI: 10.15406/mojabb.2026.10.00242

Owing to the above-mentioned assumptions, the governing equations for the biomagnetic viscoelastic fluid are taken as

$$\frac{\partial u}{\partial x}+\frac{\partial v}{\partial y}=0, \tag{1}$$

$$\rho\left(\frac{\partial u}{\partial t}+u\frac{\partial u}{\partial x}+v\frac{\partial u}{\partial y}\right)=-\frac{\partial p}{\partial x}+\mu\left(\frac{\partial^2 u}{\partial x^2}+\frac{\partial^2 u}{\partial y^2}\right)-k_0\left[\frac{\partial^3 u}{\partial t\partial x^2}+\frac{\partial^3 u}{\partial t\partial y^2}+u\frac{\partial^3 u}{\partial x\partial y^2}-v\frac{\partial^3 u}{\partial x^2\partial y}+v\frac{\partial^3 u}{\partial y^3}-\frac{\partial u}{\partial x}\frac{\partial^2 u}{\partial x^2}-\frac{\partial u}{\partial x}\frac{\partial^2 u}{\partial y^2}-\frac{\partial u}{\partial y}\frac{\partial^2 v}{\partial y^2}\right] \tag{2}$$
$$-2\left[\left(\frac{\partial u}{\partial x}\frac{\partial^2 u}{\partial x^2}+\frac{\partial v}{\partial y}\frac{\partial^2 u}{\partial y^2}+\frac{\partial u}{\partial y}\frac{\partial^2 u}{\partial x\partial y}+\frac{\partial v}{\partial x}\frac{\partial^2 u}{\partial x\partial y}\right)\right]+\mu_0 M\frac{\partial H}{\partial x},$$

$$\rho\left(\frac{\partial v}{\partial t}+u\frac{\partial v}{\partial x}+v\frac{\partial v}{\partial y}\right)=-\frac{\partial p}{\partial y}+\mu\left(\frac{\partial^2 v}{\partial x^2}+\frac{\partial^2 v}{\partial y^2}\right)-k_0\left[u\frac{\partial^3 v}{\partial x^3}+u\frac{\partial^3 v}{\partial x\partial y^2}+v\frac{\partial^3 v}{\partial x^2\partial y}+v\frac{\partial^3 v}{\partial y^3}-\frac{\partial v}{\partial x}\frac{\partial^2 u}{\partial x^2}-\frac{\partial v}{\partial x}\frac{\partial^2 u}{\partial y^2}-\frac{\partial v}{\partial y}\frac{\partial^2 v}{\partial x^2}-\frac{\partial v}{\partial y}\frac{\partial^2 v}{\partial y^2}\right] \tag{3}$$
$$-2\left[\left(\frac{\partial u}{\partial x}\frac{\partial^2 v}{\partial x^2}+\frac{\partial v}{\partial y}\frac{\partial^2 v}{\partial y^2}+\frac{\partial u}{\partial y}\frac{\partial^2 v}{\partial x\partial y}+\frac{\partial v}{\partial x}\frac{\partial^2 v}{\partial x\partial y}\right)\right]+\mu_0 M\frac{\partial H}{\partial y},$$

$$C_p\left(\frac{\partial T}{\partial t}+u\frac{\partial T}{\partial x}+v\frac{\partial T}{\partial y}\right)+\mu_0 T\frac{\partial M}{\partial t}\left(u\frac{\partial H}{\partial x}+v\frac{\partial H}{\partial y}\right)=k\left(\frac{\partial^2 T}{\partial x^2}+\frac{\partial^2 T}{\partial y^2}\right)$$
$$+\mu\left[2\left(\frac{\partial u}{\partial x}\right)^2+2\left(\frac{\partial v}{\partial y}\right)^2+\left(\frac{\partial v}{\partial x}+\frac{\partial u}{\partial y}\right)^2\right]-k_0\frac{\partial u}{\partial y}\frac{\partial}{\partial y}\left(u\frac{\partial u}{\partial x}+v\frac{\partial u}{\partial y}\right), \tag{4}$$

The boundary conditions for the present problem are mathematically described as

$$u=U_w=cxe^{i\omega t}, v=0, T=\theta T_w e^{i\omega t}, p+\frac{\rho\left(u^2+v^2\right)}{2}=0 \text{ at } y=h, \tag{5}$$

$$\frac{\partial u}{\partial y}=0, v=0, \frac{\partial T}{\partial y}=0 \text{ at } y=0. \tag{6}$$

In the aforementioned equations, u and v denote the fluid velocity components along the x and y axes, respectively. The variable p signifies the pressure, ρ is the density of the biomagnetic fluid, and μ indicates its dynamic viscosity. The parameter c_p stands for the specific heat at constant pressure, k is the thermal conductivity, and H represents the intensity of the applied magnetic field. The coefficient k_0 characterizes the viscoelastic nature of the fluid, c is the stretching rate, and ω refers to the angular frequency of wall oscillation.

The magnetic body force components per unit volume are expressed by the terms $\mu_0 M\frac{\partial H}{\partial x}$ and $\mu_0 M\frac{\partial H}{\partial y}$ in equations (2) and (3), where μ_0 is the magnetic permeability and M is the magnetization of the fluid. In the thermal energy equation (4), the second term on the left-hand side corresponds to the thermal energy generated per unit volume due to the magnetization process, which is considered adiabatic in nature. In viscoelastic fluid motion, energy is partitioned between storage and dissipation—part of it is stored as elastic (strain) energy, while the remainder is lost due to viscous effects. This is reflected in equation (4), where the second and third terms on the right-hand side represent viscous dissipation and the storage of strain energy, respectively.

The response of a biomagnetic fluid under a magnetic field is governed by its magnetization M, which is defined as the magnetic moment per unit volume. At equilibrium, the magnetization depends on variables such as temperature, fluid density, and the strength of the applied magnetic field. A fundamental relation describing the dependence of magnetization M on temperature T was proposed by Andersson and Valnes,[22] and is expressed as:

$$M=K_1 T, \tag{7}$$

where K_1 is a constant called the pyromagnetic coefficient. The biomagnetic fluid flow is influenced by the magnetic field generated by the magnetic dipole, whose magnetic scalar potential can be expressed as follows (cf.):[44,45]

$$\phi=\frac{\gamma}{2\pi}.\frac{x}{x^2+(y-d)^2}, \tag{8}$$

where $d=h+a$, and γ signifies the magnetic field strength situated at the source $(0,d)$ as illustrated in Figure 1.

The components of the magnetic field H are given by

$$H_x=-\frac{\partial\phi}{\partial x}=\frac{\gamma}{2\pi}.\frac{x^2-(y-d)^2}{\left[x^2+(y-d)^2\right]^2}, \tag{9}$$

$$H_y=-\frac{\partial\phi}{\partial y}=\frac{\gamma}{2\pi}\frac{2x(y-d)}{\left[x^2+(y-d)^2\right]^2}. \tag{10}$$

Thus, we write the magnitude of the magnetic field H as

$$H(x,y)=\sqrt{H_x^2+H_y^2}=\frac{\gamma}{2\pi}.\frac{1}{x^2+(y-d)^2}. \tag{11}$$

Analytical derivation

To solve the system of governing equations (2)-(4) for biomagnetic fluid flow, subject to the boundary conditions (5) and (6), along with the relations (7) and (11), we begin by introducing the following dimensionless variables:

$$\psi(\xi,\eta)=h^2 c\xi f(\eta)e^{i\omega t}, \tag{12}$$

$$P(\xi,\eta)=\frac{p}{c\mu}=-\left(P_1(\eta)+\xi^2 P_2(\eta)\right)e^{i\omega t}, \tag{13}$$

$$\theta(\eta)=\frac{T}{T_w}=\left(\theta_1(\eta)+\xi^2\theta_2(\eta)\right)e^{i\omega t}, \tag{14}$$

and the non-dimensional coordinates

$$\xi = \frac{x}{h}, \eta = \frac{y}{h}, \tau = \omega t, \tag{15}$$

where the stream function, temperature and pressure variables are denoted by $\psi(\xi,\eta)$, $\mathrm{P}(\xi,\eta)$ and $\theta(\xi,\eta)$, respectively.

The velocity components u and v in terms of the non-dimensional stream function can be obtained as

$$u = \frac{\partial \psi}{\partial y} = cxe^{i\omega t} f'(\eta), \tag{16}$$

$$v = -\frac{\partial \psi}{\partial x} = -hce^{i\omega t} f(\eta). \tag{17}$$

Here, the velocity components u and v satisfy the continuity equation (1) automatically. By the use of equations (12)-(17) into the equations (2)-(4) and then equating the coefficients of like powers of ξ, we obtain the following system of ordinary differential equations:

$$f''' - \mathrm{Re}\left(f'^2 - ff''\right)\cos\tau - K\cos\tau\left(2f'f''' - f''^2 - ff^{iv}\right) + 2P_2\cos\tau - \frac{2Bm\theta_1}{\mathrm{Re}(\eta-\alpha)^4} = 0, \tag{18}$$

$$f'' + ff' + K\left(ff''' - 3f'f''\right) + \frac{2Bm\theta_1}{(\eta-\alpha)^3} - P'_1 = 0, \tag{19}$$

$$\frac{2Bm\cos\tau\theta_2}{\mathrm{Re}(\eta-\alpha)^3} - \frac{4Bm\cos\tau\theta_1}{\mathrm{Re}(\eta-\alpha)^5} - P'_2 = 0, \tag{20}$$

$$\theta''_1 + P_r\,\mathrm{Re}\cos\tau f\theta'_1 - \frac{2Bm\lambda f\cos\tau}{(\eta-\alpha)^3}\theta_1 + 2\theta_2 + 4\,\mathrm{Re}\,\lambda\cos\tau f'^2 = 0, \tag{21}$$

and

$$\theta''_2 + \mathrm{Pr}\,\mathrm{Re}\cos\tau f\theta'_2 - 2\,\mathrm{Pr}\,\mathrm{Re}\cos\tau\theta_2 f' + \frac{2Bm\lambda f'\cos\tau}{(\eta-\alpha)^4}\theta_1 + \frac{4Bm\lambda f\cos\tau}{(\eta-\alpha)^5}\theta_1 + \mathrm{Re}\,\lambda\cos\tau f''^2 - \frac{2Bm\lambda f\cos\tau}{(\eta-\alpha)^3}\theta_2 - K\lambda\,\mathrm{Re}\cos 2\tau\left[f'f''^2 - ff''f'''\right] = 0, \tag{22}$$

In the same way, the boundary conditions (5) and (6), subject to the transformations (12)-(17), yield

$$f''(0) = 0, f(0) = 0, \theta'_1(0) = 0, \theta'_2(0) = 0, \tag{23}$$

$$f(1) = 0,\ f'(1) = 1,\ \theta_1(1) = 1,\ \theta_2(1) = 0,\ P_1(1) = 0,\ P_2(1) = \frac{1}{2}\mathrm{Re}, \tag{24}$$

where the prime denotes ordinary differentiation with respect to η only, $K = \frac{K_0 c}{\rho\nu}$ is the viscoelastic parameter, $Bm = \frac{\nu}{2\pi}\frac{\mu_0 k_1 T_w \rho}{\mu^2}$ the ferromagnetic interaction parameter, $P_r = \frac{\mu C_p}{k}$ the Prandtl number, $\mathrm{Re} = \frac{c\rho h^2}{\mu}$ the Reynolds number, $\lambda = \frac{c\mu^2}{\rho T_w}$ the viscous dissipation parameter and $S = \frac{\omega}{c}$ represents a non-dimensional variable.

Due to the strong nonlinearity of equation (18) and the assumption of a small viscoelastic parameter, we employ a perturbation technique to obtain an approximate solution. Accordingly, the solution is expanded as follows:

$$f = f_0(\eta) + Kf_1(\eta) + K^2 f_1(\eta) + \cdots. \tag{25}$$

Substituting (25) into Eq. (18), equating the like powers of K while neglecting quadratic and higher-order terms, we obtain:

$$f_0''' - \mathrm{Re}\cos\tau\left(f_0'^2 - f_0 f_0''\right) + 2\cos\tau P_2 - \frac{2Bm\theta_1}{\mathrm{Re}(\eta-\alpha)^4} = 0, \tag{26}$$

and

$$f_1''' - \mathrm{Re}\cos\tau\left(2f_0'f_1' - f_1f_0'' - f_0f_1''\right) - \cos\tau\left(2f_0'f_0''' - f_0f_0^{iv} - f_0''^2\right) = 0. \tag{27}$$

Using (25), the boundary conditions for f_0 and f_1 from (23) and (24) can be written as

$$f_0(0) = 0, f_0''(0) = 1; f_0(1) = 0, f'_0(1) = 1, \tag{28}$$

$$f_1(0) = f_1''(0) = 0; f_1(1) = 0,\ f'_1(1) = 0. \tag{29}$$

The set of coupled ordinary differential equations (18) to (22), together with the boundary values (23) and (24), is solved by developing an appropriate computational procedure. It is worthwhile to mention here that according to equation (13), the pressure variable P_1 is present only in Equation (19), while Equations (18) and (20) to (22) are independent of P_1. This allows us to exclude P_1 from further consideration when the objective is to study the velocity field.

Computational procedure

To numerically solve equations (26) and (27) subject to the boundary conditions (28) and (29), we implement a finite difference scheme incorporating Newton's linearization approach, as described below:

Substituting $f' = F$ in (26) and (28), we have Equations (26) and (27), together with boundary conditions (28) and (29), are solved using a finite-difference method integrated with Newton's linearization procedure, as detailed below:

By substituting $f' = F$ in equations (26) and (28), we obtain:

$$F'' - \mathrm{Re}\left(F^2 - f_0F'\right)\cos\tau + 2P_2\cos\tau - \frac{2Bm\theta_1}{\mathrm{Re}(\eta-\alpha)^4} = 0, \tag{30}$$

$$F'(0) = 0, F(1) = 1. \tag{31}$$

Using the following central differences for the first and second-order derivatives with respect to η, we write

$$(F')_i = \frac{F_{i+1} - F_{i-1}}{2\delta\eta} + O\left((\delta\eta)^2\right), \tag{32}$$

and

$$(F'')_i = \frac{F_{i+1} - 2F_i + F_{i-1}}{(\delta\eta)^2} + O\left((\delta\eta)^2\right), \tag{33}$$

where i represents the mesh index in the η-direction with $\eta_i = i * \delta\eta$; $i = 0,1,\cdots m$, and $\delta\eta$ is the spacing length along the η-axis.

Once the dependent variables are evaluated at the nth iteration, their updated values for the next $(n+1)$th iteration are computed using the following iterative relation:

$$F_i^{n+1} = F_i^n + (\Delta F_i)^n, \qquad (34)$$

In this context, $(\Delta F_i)^n$ denotes the error at the nth iteration for each grid point $i = 0,1,2,\cdots,m$. Notably, the error at the boundary points is zero since the boundary values of F_i are prescribed and remain fixed throughout the computation.

Given the strong nonlinearity of equation (26), it is solved numerically for f using the finite difference method described earlier. Once the numerical solution for f is obtained, we then proceed to solve equations (20)–(22), subject to the boundary conditions (23) and (24), by applying a suitable finite difference scheme.

Results and discussion

In this section, we demonstrate the practical implementation of the developed mathematical model, its analytical formulation, and the numerical method introduced earlier. Our primary objective is to obtain theoretical estimates for key parameters governing blood flow in an oscillatory artery with stretching walls. For this purpose, blood is modeled as a biomagnetic fluid. The previously described numerical scheme is employed to solve the governing equations (18)–(22), subject to the appropriate boundary conditions (23) and (24). To facilitate the numerical computations, specific values must be assigned to the dimensionless parameters involved in the analysis. For the computational procedure, we used the following values: $\rho = 1050 kg/m^3$, $\mu = 3.2\times10^{-3}$ kg/m$\cdot s$. The numerical investigation aimed to examine the variations of various dimensionless parameters using the following data: ferromagnetic interaction parameter, $B_m = 0,2,3,4,6$; viscoelastic parameter, $K = 0.0,0.01,0.05,0.1$; Prandtl number, $\mathrm{Pr} = 7.0,14.0,21.0$; non-dimensional variable $S = 1.0$; dimensionless distance $\alpha = 2.5,3.0,3.5$; Reynolds number $\mathrm{Re} = 1,2,3,4$; and viscous dissipation parameter $\lambda = 0.01$. The computational work was carried out using a grid spacing of $\delta\eta = 0.0125$. It was observed that further reduction in the value of $\delta\eta$ resulted in negligible changes in the computed results, indicating numerical convergence. The outcomes of the simulations are presented graphically in Figures 2–13.

To validate the numerical results of the present study, the velocity profiles depicted in Figures 2(a) & 2(b) under the influence of a magnetic field were compared with those reported in previously published and widely cited scientific literature.[27]

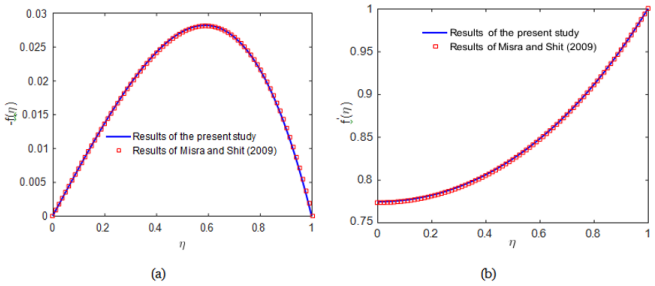

Figure 2 Comparison of (a) normal component of velocity $-f$ (η) and (b) axial velocity f'(η) with the results of Misra and Shit (2009), when *Bm* = 2.0, *Re* = 1.0, *K* = 0.0, *Pr*= 21.0, τ = 0, *S* = 1.0, λ = 0.01, α = 2.5.

Figures 3 to 5 illustrate the variation of the axial velocity component $f'(\eta)$ with respect to the transverse coordinate η, for different values of the dimensionless parameters. Figure 3 demonstrates the influence of the ferromagnetic interaction parameter B_m on the axial velocity. As B_m increases, the velocity near the centerline of the channel decreases, while it attains a maximum at the wall due to the stretching effect. This implies that an external magnetic field induced by a magnetic dipole can significantly enhance flow velocity near the channel walls while suppressing it at the core. Figure 4 shows the effect of the viscoelastic parameter K, indicating that the axial velocity decreases in the central region with increasing K, but exhibits a reverse trend near the boundaries. This behavior highlights the role of blood's non-Newtonian and viscoelastic characteristics in reducing flow velocity, particularly within the core region. Figure 5 illustrates the impact of the dimensionless distance α from the magnetic dipole source. A noticeable change in axial velocity is observed between $\alpha = 2.5$ and $\alpha = 3$; beyond this range, further variations are negligible. The observed increase in blood velocity with greater distance from the magnetic dipole can be attributed to the rapid attenuation of the magnetic field strength. As the distance from the dipole increases, the intensity and gradient of the magnetic field diminish significantly, thereby reducing the opposing magnetic force exerted on the biomagnetic fluid. This reduction in magnetic resistance leads to diminished damping effects, allowing the blood to flow more freely and resulting in an increase in axial velocity. This indicates a saturation effect in magnetic influence as the distance from the dipole increases. It is important to note that the behavior observed in the present results differs significantly from that reported in the earlier study by Raju et al.,[27] primarily due to the consideration of oscillatory flow in the current analysis. Nonetheless, both studies show agreement at the initial time $t = 0$.

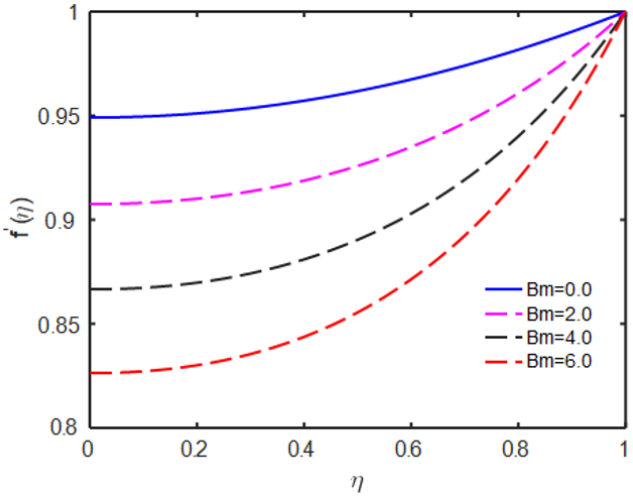

Figure 3 Variation of axial velocity component f'(η) with η for different values of *Bm*, when *Pr* = 21.0, *Re* = 2.0, *K* = 0.01, *S* = 1.0, λ = 0.01, α = 2.5, τ = 5π/2. Due to the stretching of the wall, the velocity at the wall dominates the adjacent fluid motion, resulting in a lower fluid velocity at the central line.

Figures 6 to 8 depict the distribution of the non-dimensional temperature $\theta_1(\eta)$ as a function of the transverse coordinate η at time $\tau = \frac{5\pi}{2}$. As shown in Figure 6, the temperature $\theta_1(\eta)$ increases with an increase in the ferromagnetic interaction parameter B_m, indicating enhanced thermal conduction due to magnetic effects. Similarly, Figure 7 demonstrates that a higher Prandtl number P_r also leads to an increase in temperature, reflecting the dominance of thermal diffusion over momentum diffusion. In contrast, Figure 8 reveals that the temperature decreases with increasing values of the viscoelastic parameter K, suggesting that viscoelastic effects suppress thermal transport within the fluid. Across all three cases, it is observed that the temperature consistently decreases from the channel walls toward the centerline, highlighting the effect of thermal boundary layers. Figure 9 presents the variation of the dimensional pressure P_2 for different

Citation: Haldar R, Shit GC, Misra JC. Oscillatory flow of a bio-magnetic viscoelastic fluid in a channel with stretching walls. *MOJ App Bio Biomech.* 2026;10(1):60–61. DOI: 10.15406/mojabb.2026.10.00242

values of the ferromagnetic interaction parameter B_m. The results indicate that pressure decreases as the magnetic field strength increases. However, under the influence of a magnetic field, the dimensionless pressure remains uniform and equal to unity throughout the channel height.

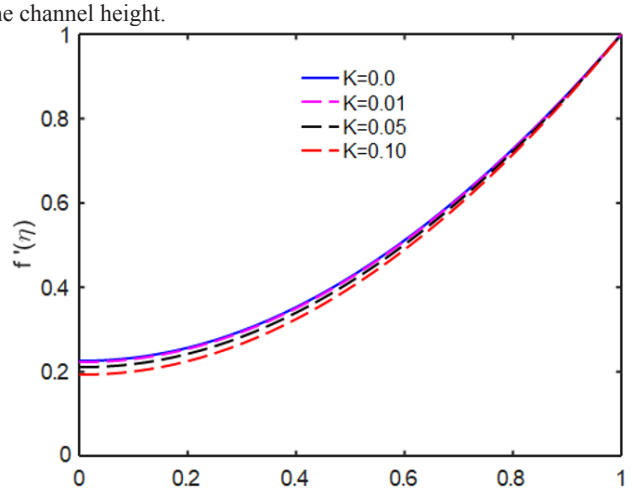

Figure 4 Variation of $f'(\eta)$ with η for different values of *K*, when *Pr* = 21.0, *Re* = 2.0, *Bm* = 2.0, *S* = 1.0, λ = 0.01, α = 2.5, τ = 5*π*/2.

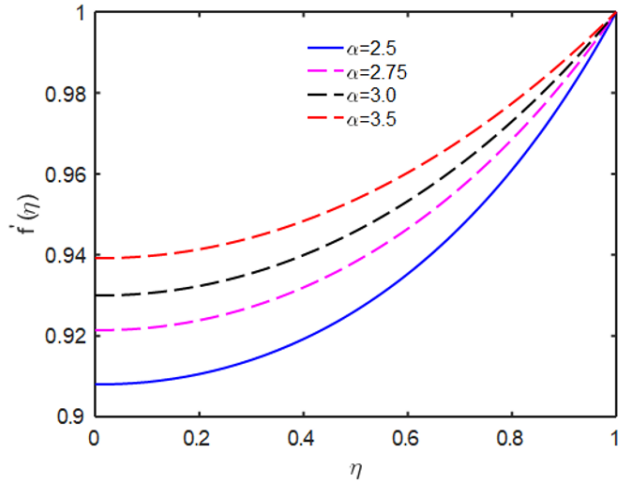

Figure 5 Variation of $f'(\eta)$ with η for different values of α, when *Pr* = 21.0, *Re* = 2.0, *Bm* = 2.0, *K* = 0.01, *S* = 1.0, λ = 0.01, τ = 5*π*/2.

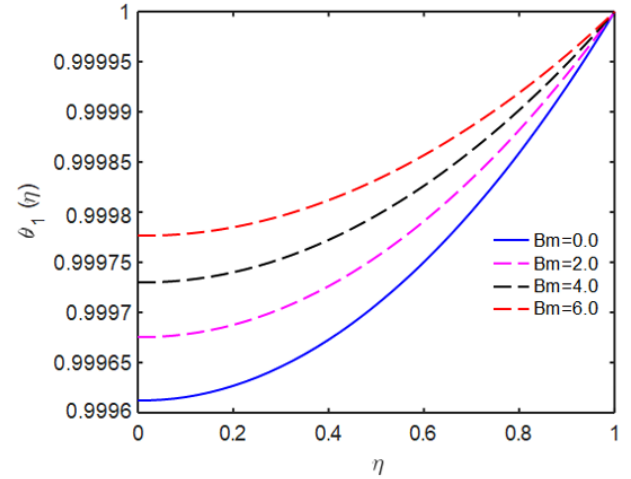

Figure 6 Variation of dimensionless temperature $\theta_1(\eta)$ with η for different values of *Bm*, when *Pr* = 21.0, *Re* = 2.0, *K* = 0.01, *S* = 1.0, λ = 0.01, α = 2.5, τ = 5*π*/2.

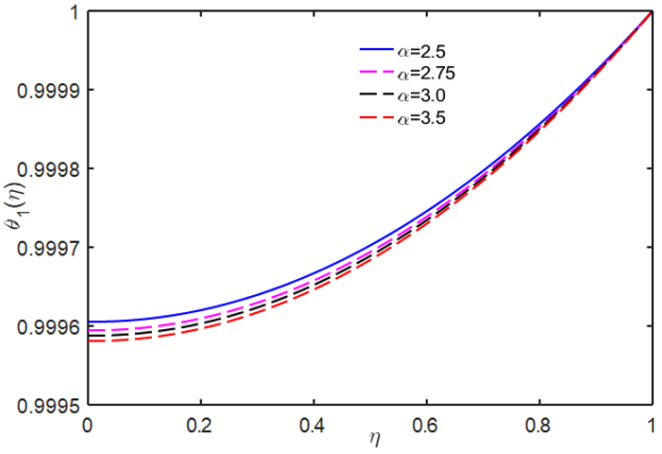

Figure 7 Variation of dimensionless temperature $\theta_1(\eta)$ with η for different values of α, when*Re* = 2.0, *Bm* = 2.0, *K* = 0.01, *Pr* = 21.0, *S* = 1.0, λ = 0.01, τ = 5*π*/2.

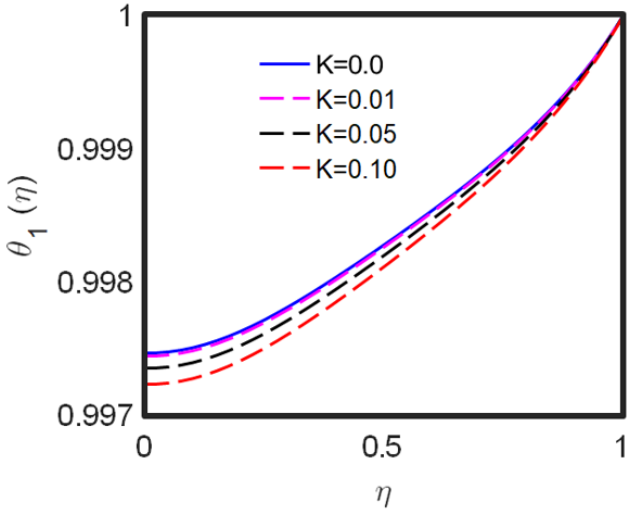

Figure 8 Variation of dimensionless temperature $\theta_1(\eta)$ with η for different values of *K*, when *Re* = 2.0, *Bm* = 2.0, *K* = 0.01, *Pr* = 21.0, *S* = 1.0, λ = 0.01, τ = 5*π*/2.

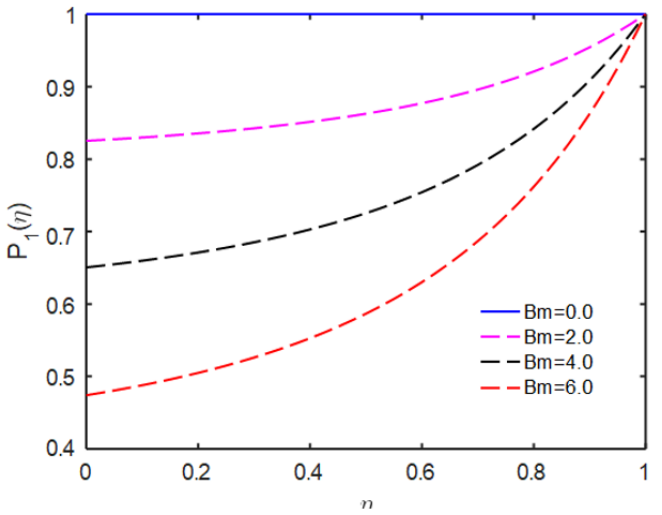

Figure 9 Variation of P_1 with η for different values of *Bm*, when *Pr* = 21.0, *Re* = 2.0, *K* = 0.01, *S* = 1.0, λ = 0.01, α = 2.5, τ = 5*π*/2.

Citation: Haldar R, Shit GC, Misra JC. Oscillatory flow of a bio-magnetic viscoelastic fluid in a channel with stretching walls. *MOJ App Bio Biomech.* 2026;10(1):60–61. DOI: 10.15406/mojabb.2026.10.00242

Figures 10 & 11 illustrate the temporal variation of the axial velocity component at the channel wall and at the centerline, respectively. These figures clearly demonstrate that the axial velocity exhibits oscillatory behavior throughout the channel over time. A key observation is that the amplitude of these oscillations diminishes with increasing values of the ferromagnetic interaction parameter B_m, indicating a damping effect induced by the magnetic field. Furthermore, both figures show that the time-averaged axial velocity remains positive at both the wall and the centerline for all considered values of B_m, suggesting a net forward flow despite the oscillatory nature. It is also noteworthy that the amplitude of velocity oscillations is significantly higher at the centerline compared to the channel wall, reflecting the influence of wall stretching and boundary layer effects.

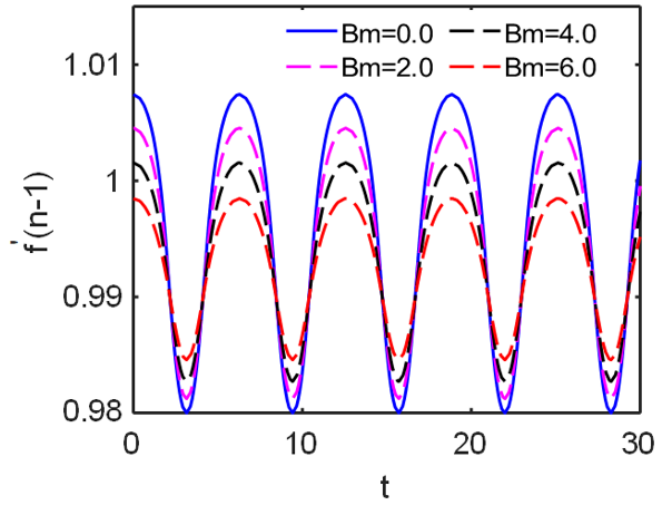

Figure 10 Variation of $f'(n-1)$ with τ for different values of *Bm*, when *Pr* = 21.0, *Re*= 2.0, *K* = 0.01, *S* = 1.0, λ = 0.01, α = 2.5.

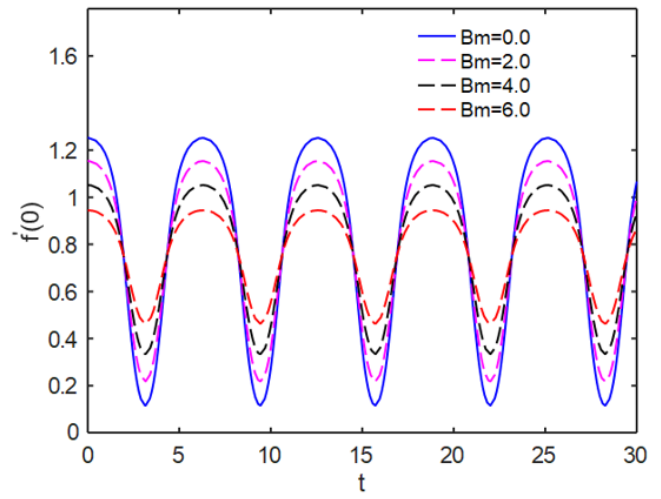

Figure 11 Variation of $f'(1)$ with τ for different values of *Bm*, when *Pr* = 21.0, *Re* = 2.0, *K* = 0.01, *S* = 1.0, λ = 0.01, α = 2.5.

The key feature of this investigation is the local skin-friction coefficient C_f, which is defined by

$$C_f = \frac{\tau_w}{\rho U^2} = \frac{1}{\mathrm{Re}}\left[1 - 3K\cos\omega t\right] f''(1), \quad (35)$$

in which τ_w is the wall skin-friction given by

$$\tau_w = \mu\left(\frac{\partial u}{\partial y}\right)_{y=h} - K_0\left[u\left(\frac{\partial^2 u}{\partial x \partial y} + \frac{\partial^2 v}{\partial x^2}\right) + v\left(\frac{\partial^2 u}{\partial y^2} - \frac{\partial^2 u}{\partial x^2}\right) + 2\frac{\partial u}{\partial x}\frac{\partial u}{\partial y} - 2\frac{\partial v}{\partial x}\frac{\partial u}{\partial y} + \frac{\partial^2 u}{\partial t \partial y}\right]_{y=h}. \quad (36)$$

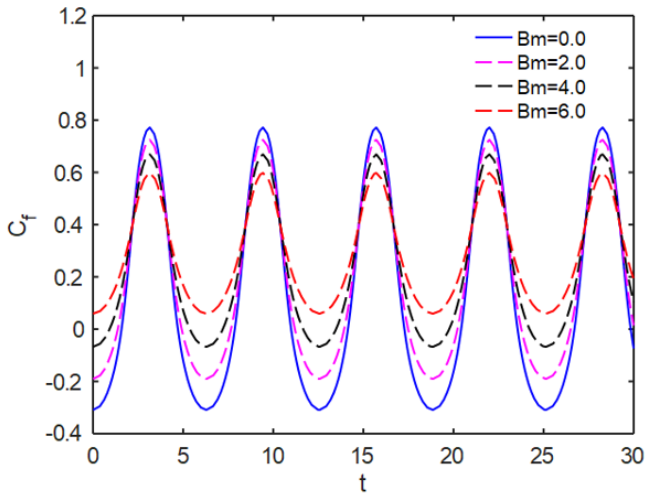

Figure 12 Variation of Skin-friction C_f with τ for different values of *Bm*, when *Pr* = 21.0, *Re* = 2.0, *K* = 0.01, *S* = 1.0, λ = 0.01, α = 2.5.

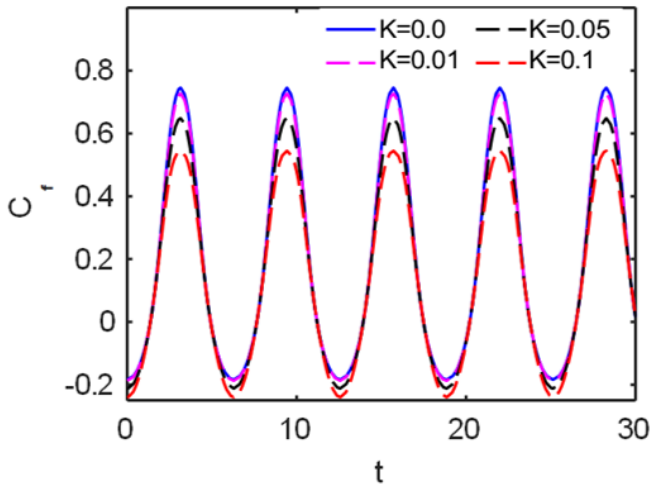

Figure 13 Variation of Skin-friction C_f with τ for different values of *K*, when *Pr* = 21.0, *Re* = 2.0, *Bm* = 2.0, *S* = 1.0, λ = 0.01, α = 2.5.

The most notable feature that warrants special attention is the periodic patterns observed in the skin-friction coefficient C_f, as shown in Figures 11 & 12. Figures 12 & 13 illustrate how the skin-friction coefficient C_f varies over time τ for different values of the ferromagnetic interaction parameter B_m and the viscoelasticity parameter K. It is evident that the skin-friction coefficient C_f exhibits periodic oscillations over time τ. Furthermore, Figures 12 & 13 indicates that the amplitude of these oscillations decreases as the ferromagnetic parameter B_m and the viscoelasticity parameter K increase.

When shear stress on a vessel wall is high, it can cause damage to the wall, resulting in intimal thickening. This can occur when blood

viscoelasticity is significantly high. Conversely, if the wall shear stress is low, it facilitates mass transport, leading to an accumulation of erythrocytes near the wall.

Conclusion

We have investigated the oscillatory flow behavior of a biomagnetic viscoelastic fluid in a channel with stretching walls, subjected to an external magnetic field generated by a magnetic dipole. For modeling purposes, blood is treated as a biomagnetic fluid. The dimensionless parameters used in the numerical simulations are chosen based on experimentally reported values for blood, as available in the literature. A significant reduction in blood velocity near the channel centerline is observed, primarily attributed to the elastic nature of the vessel walls.

The key findings of this study are summarized below:

Axial velocity decreases with an increase in the ferromagnetic interaction parameter B_m .

Viscoelastic effects of blood lead to a further reduction in axial velocity. While the blood temperature increases with stronger magnetic fields, it decreases with increasing viscoelasticity.

Axial velocity and the skin-friction coefficient exhibit periodic oscillations over time.

Oscillation amplitude diminishes with increasing values of both the ferromagnetic interaction parameter B_m and the viscoelastic parameter K .

The insights gained from this study are likely to possess potential applications in biomedical engineering, such as targeted drug delivery, tissue engineering, and industrial processes involving ferrofluid thin films, including lubrication and coating technologies.

Acknowledgements

The authors thank the esteemed reviewers for their valuable comments and suggestions, which have improved the present work. This research is financially supported by the DST FIST project (Ref. No. SR/FST/ MS-II/2021/101(C)), Govt. of India.

Funding

None.

Conflicts of interest

The authors declare that there is no conflicts of interest.

References

1. Rosensweig RE. *Ferrohydrodynamics*. Cambridge University Press; 1985.
2. Bhandari A, Parmar KPS. Exploring slip effects of ferrofluid film flow over a slanted rough surface. *J Fluid Mech.* 2024;982:A19.
3. Ruuge EK, Rusetski AN. Magnetic fluids as drug carriers: Targeted transport of drugs by a magnetic field. *J Magn Magn Mater*. 1993;122:335–339.
4. Higashi T, Yamagishi A, Takeuchi T, et al. Orientation of erythrocytes in a strong static magnetic field. *Blood.* 1993;82(4):1328–1334.
5. Shaylgin AN, Norina SB, Kondorsky EI. Behavior of erythrocytes in high gradient magnetic field. *J Magn Magn Mater*. 1983;31:555–556.
6. Takeuchi T, Mizuno T, Yamagishi A, et al. Orientation of red blood cells in high magnetic field. *J Magn Magn Mater*. 1995;140-144(2):1462–1463.
7. Higashi T, Ashida N, Takeuchi T. Orientation of blood cells in a static magnetic field. *Physica B*. 1997:616–620.
8. Pauling L, Coryell CD. The magnetic properties and structure of hemoglobin, oxyhemoglobin and carbonmonoxy hemoglobin. *Proc Natl Acad Sci U S A*. 1936;22:210–216.
9. Haik Y, Chen JC, Pai VM. *Development of bio-magnetic fluid dynamics*. In: Proceedings of the IX International Symposium on Transport Properties in Thermal Fluids Engineering; June 25–28, 1996; Singapore. Hawaii, USA: Pacific Center of Thermal Fluid Engineering; 121–126.
10. Haik Y, Pai V, Chen CJ. Development of magnetic device for cell separation. *J Magn Magn Mater*. 1999;194(1-3):254–261.
11. Haik Y, Pai V, Chen CJ. Biomagnetic fluid dynamics. In: Shyy W, Narayanan R, editors. *Fluid Dynamics at Interfaces*. Cambridge University Press; 1999:439–452.
12. Jumana SA, Murtaza MG, Tzirtzilakis EE, et al. Biomagnetic flow with magnetic particles over a continuously moving sheet affected by a magnetic dipole. *Commun Nonlinear Sci Numer Simul.* 2024;138:108132.
13. Jumana SA, Ferdows M, Murtaza MG, et al. Dual solution of convective biomagnetic fluid through permeable moving flat plate considering wall transpiration and magnetization. *J Mech Med Biol*. 2023;23:2350009.
14. Ferdows M, Alam J, Murtaza MG, et al. Effects of magnetic particles diameter and particle spacing on biomagnetic flow and heat transfer over a linear/nonlinear stretched cylinder in the presence of magnetic dipole. *J Mech Med Biol*. 2023;23:2350036.
15. Murtaja MG, Akter T, Tzirtzilakis EE, et al. Numerical study of biomagnetic fluid flow over an unsteady curved stretching sheet in the presence of magnetic field. *Adv Appl Fluid Mech*. 2023;30(1):35–62.
16. Murtaja MG, Misra JC, Tzirtzilakis EE, et al. Numerical study of biomagnetic Maxwell fluid past a nonlinearly stretching sheet considering magnetization and electrical conductivity. *J Mech Med Biol*. 2023;23(5):2350034.
17. Alam J, Murtaja MG, Tzirtzilakis EE, et al. Partial slip effect of Cu, Au, and TiO2 nanoparticles in steady biomagnetic fluid flow and heat transfer over a stretching sheet in the presence of magnetic dipole. *Int J Mater Eng Technol*. 2024;23:37-56.
18. Tzirtzilakis EE, Kafoussias NG. Biomagnetic fluid flow over a stretching sheet with nonlinear temperature-dependent magnetization. *Z Angew Math Phys*. 2003;54(4):551–565.
19. Tzirtzilakis EE, Xenos MA. Biomagnetic fluid flow in a driven cavity. *Meccanica.* 2013;48:187–200.
20. Tzirtzilakis EE, Xenos M, Loukopoulos VC, et al. Turbulent biomagnetic fluid flow in a rectangular channel under the action of a localized magnetic field. *Int J Eng Sci*. 2006;44:1205–1224.
21. Habibi MR, Ghassemi M, Shahidian A. Investigation on biomagnetic fluid flow under non-uniform magnetic field. *Nanoscale Microscale Thermophys Eng*. 2012;16:64–77.
22. Andersson HI, Valnes OA. Flow of a heated ferrofluid over a stretching sheet in the presence of magnetic dipole. *Acta Mech*. 1998;128(1-2):39–47.
23. Fukada E, Kaibara M. Viscoelastic study of aggregation of red blood cells. *Biorheology*. 1980;17(1-2):177–182.
24. Thurston GB. Viscoelasticity of human blood. *Biophys J*. 1972;12(9):1205–1217.
25. Stoltz JF, Lucius M. Viscoelasticity and thixotropy of human blood. *Biorheology*. 1981;18(3–6):453–473.
26. Misra JC, Shit GC. Biomagnetic viscoelastic fluid flow over a stretching sheet. *Appl Math Comput.* 2009;210(2):350–361.

27. Misra JC, Shit GC. Flow of a biomagnetic viscoelastic fluid in a channel with stretching walls. *J Appl Mech*. 2009;76(6):061006.
28. Misra JC, Sinha A, Shit GC. Flow of a biomagnetic viscoelastic fluid: Application to estimation of blood flow in arteries during electromagnetic hyperthermia. *Appl Math Mech (Engl Ed)*. 2010;31(11):1405–1420.
29. Datti PS, Prasad KV, Abel MS, et al. MHD viscoelastic fluid flow over a non-isothermal stretching sheet. *Int J Eng Sci.* 2004;42:935–946.
30. Cortell R. A note on flow and heat transfer of a viscoelastic fluid over a stretching sheet. *Int J Non Linear Mech.* 2006;41:78–85.
31. Rajagopal KR, Na TY, Gupta AS. Flow of a viscoelastic fluid over a stretching sheet. *Rheol Acta.* 1984;24:213–215.
32. Andersson HI, Bech KH, Dandapat BS. Magnetohydrodynamic flow of a power-law fluid over a stretching sheet. *Int J Non Linear Mech.* 1992;27:929–936.
33. Andersson HI, Dandapat BS. Flow of a power-law fluid over a stretching sheet. *Stability Appl Anal Continuous Media.* 1991;1:339–347.
34. Misra JC, Pal B, Gupta AS. Hydromagnetic flow of a second-grade fluid in a channel: Some applications to physiological systems. *Math Models Methods Appl Sci.* 1998;8:1323–1342.
35. Misra JC, Pal B. Hydromagnetic flow of a viscoelastic fluid in a parallel plate channel with stretching walls. *Indian J Math*. 1999;41:231-247.
36. Misra JC, Shit GC, Rath HJ. Flow and heat transfer of a MHD viscoelastic fluid in a channel with stretching walls: Some applications to haemodynamics. *Comput Fluids.* 2008;37:1–11.
37. Nadeem S, Akbar NS, Hayat T, et al. Influence of heat and mass transfer on Newtonian biomagnetic fluid of blood flow through tapered porous arteries with a stenosis. *Transp Porous Media.* 2012;91:81–100.
38. Ramachandra Rao, Desikachar KS. MHD oscillatory flow of blood through channels of variable cross-section. *Int J Eng Sci.* 1986;24:1615–1628.
39. Oleson JR, Sim DA, Manning MR. Analysis of prognostic variables in hyperthermia treatment of 161 patients. *Int J Radiat Oncol Biol Phys.* 1984;10:2231–2239.
40. Reinhold HS, Endrich B. Tumor microcirculation as a target for hyperthermia. *Int J Hyperthermia.* 1986;2:111–137.
41. Womersley JR. Oscillatory motion of a viscous liquid in a thin-walled elastic tube. I. The linear approximation for long waves. *Philos Mag.* 1955;46:199–221.
42. Uchida S. The pulsating viscous flow superimposed on the steady laminar motion of incompressible fluid in a circular pipe. *Z Angew Math Phys*. 1956;7:403–422.
43. Craciunescu OI, Clegg CT. Pulsatile blood flow effects on temperature distribution and heat transfer in rigid vessels. *J Biomech Eng.* 2001;123:500–505.
44. Tzirtzilakis EE, Tanoudis GB. Numerical study of biomagnetic fluid flow over a stretching sheet with heat transfer. *Int J Numer Methods Heat Fluid Flow*. 2003;13(7):830–848.
45. Andersson HI, Valnes OA. Flow of a heated ferrofluid over a stretching sheet in the presence of a magnetic dipole. *Acta Mech.* 1998;128:39–47.

Citation: Haldar R, Shit GC, Misra JC. Oscillatory flow of a bio-magnetic viscoelastic fluid in a channel with stretching walls. *MOJ App Bio Biomech.* 2026;10(1):60–61. DOI: 10.15406/mojabb.2026.10.00242